Chest electrical impedance tomography examination, data analysis, terminology, clinical use and recommendations: consensus statement of the TRanslational EIT developmeNt stuDy group

Inéz Frerichs, Marcelo B. P. Amato, Anton H. van Kaam, David G. Tingay, Zhanqi Zhao, Bartłomiej Grychtol, Marc Bodenstein, Hervé Gagnon, Stephan H. Böhm, Eckhard Teschner, Ola Stenqvist, Tommaso Mauri, Vinicius Torsani, Luigi Camporota, Andreas Schibler, Gerhard K. Wolf, Diederik Gommers, Steffen Leonhardt, Andy Adler, TREND study group

ONLINE SUPPLEMENT 4

Functional EIT images

Functional EIT images

This electronic online supplement (EOS) describes how functional EIT (fEIT) images are generated from raw EIT images (and, in some cases, also using other physiological signals recorded in parallel during the EIT examination). An fEIT image is generated from a mathematical operation on a sequence of raw EIT images and the resulting EIT waveforms. The mathematical operations determine the type of fEIT image, and are designed to measure specific regional physiological characteristics, such as delay in local ventilation onset or regional respiratory system compliance (C_{rs}). Figure E4.1 shows the sequence of all processes involved in EIT examinations and the place of fEIT images in this scheme.

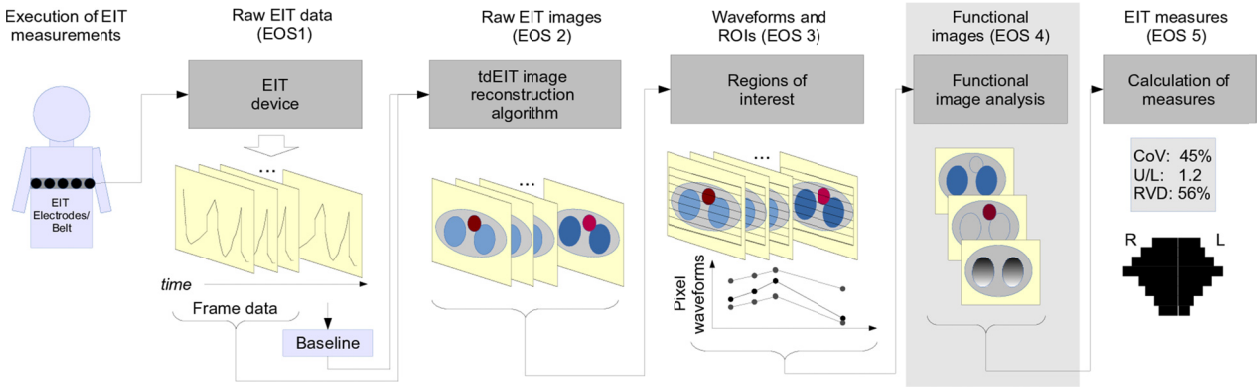

Figure E4.1. Sequence of processes involved in EIT chest examination and data analysis. EOS 4 (gray background) describes the generation of functional EIT images. Abbreviations: EOS, electronic online supplement; tdEIT, time-difference EIT; ROI, region-of-interest; CoV, center of ventilation; U/L, upper-to-lower ventilation ratio; RVD, regional ventilation delay; R, right; L, left.

General principle of functional EIT imaging

EIT is an imaging technique with a high temporal resolution that can quickly provide a very large number of raw images (EOS 2) within each breath. No single EIT image contains all the clinical information on ventilation and cardiac activity by itself. Such information is distributed over a number of raw images and requires analyzing the character, timing, speed, frequency and localization of impedance changes in a sequence of raw images.

The generation of fEIT images requires the availability of EIT waveforms (EOS 3), obtained from a sequence of raw EIT images, on which a mathematical function or an algorithm is applied to calculate a physiologically relevant parameter for each image pixel.

The result is a single new image called a functional image, The general process for generating an fEIT image is illustrated in Figure E4.2. To highlight the fact that different types of fEIT images, addressing different functional characteristics of the respiratory system, can be generated from a single EIT examination, all figures in this EOS, unless otherwise noted, are based on a single dataset (1). These data were acquired on a ventilated newborn pig using the Goe-MF II EIT device (CareFusion, Höchberg, Germany) during an incremental and decremental PEEP trial, during which both EIT and airway opening pressure were simultaneously measured.

Various types of fEIT images have been proposed in the literature and used to quantify and characterize regional lung ventilation and/or perfusion. For most types of fEIT image, it is possible to generate secondary functional images, by comparing results achieved at different times throughout an experimental or clinical interaction with the subject. Thus, for example, an image of the change in ventilation distribution after an intervention can be visualized by subtracting the fEIT images obtained before and after the intervention (2, 3). We describe some of the most common approaches to fEIT image generation in this EOS, and provide references for others, though the list is by no means comprehensive.

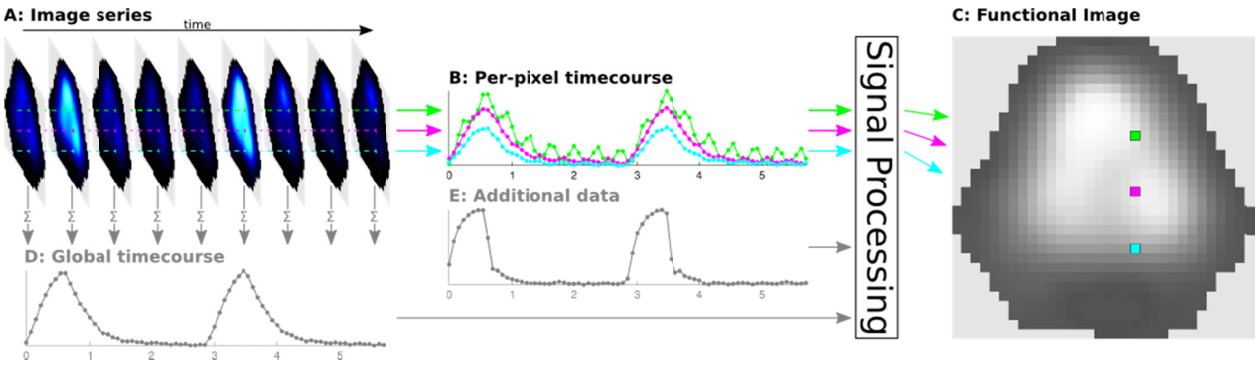

Figure E4.2. Conceptual diagram of the process of computing a functional EIT image. A) a sequence of raw EIT images is obtained (EOS 2); B) A waveform is obtained for each pixel (EOS 3) from the image sequence (A); C) Using various signal processing approaches (described in the text) a functional EIT image pixel value is calculated based on the pixel waveform (B); D) Some approaches require a global waveform (time course) that is obtained by computing the sum of all image pixels, or other auxiliary data such as pressure or volume recordings from the patient ventilator or spirometer.

Types of functional EIT images

We group fEIT imaging approaches according to their target physiological parameters: ventilation distribution, ventilation- and cardiac-frequency impedance changes, aeration change, respiratory system mechanics, ventilation timing, and tissue classification (i.e. for regions of repeated opening and closing and for overdistended and atelectatic tissue). The different approaches differ in their requirements for additional simultaneous information in addition to the EIT data (e.g. airway pressure), and specific clinical interventions (e.g. constant low-flow inflation). We conclude by describing various approaches to combine different types of fEIT image to label the state of different regions of the lung into states (e.g. atelectatic or overdistended).

Because of the variety of fEIT approaches and techniques, many different terms have been used for the same calculation. In some cases, early terminology has been replaced by more precise terms. In Table E4.1, we show the fEIT imaging categories and the associated imaging techniques. Technical details are described in subsequent sections.

Table E4.1. Overview of the various fEIT imaging techniques with older or alternative taxonomy organized by fEIT imaging categories.

fEIT imaging category	fEIT imaging technique	Alternative terms
Ventilation (distribution of)	Standard deviation fEIT	SD fEIT
	Tidal variation fEIT	V_T fEIT, TV fEIT, tidal fEIT
	Normalized tidal variation fEIT	Stretch fEIT
	fEIT of other lung volumes than V_T	FVC fEIT, FEV_1 fEIT, IVC fEIT
	fEIT of ratios of lung volumes or flows	FEV_1/FVC fEIT, FEF_{75}/FEF_{25} fEIT
Frequency analysis of impedance changes	Ventilation-frequency fEIT	
	Cardiac-frequency fEIT, Pulsatility fEIT	Cardio-synchronous fEIT, heart beat-related fEIT, perfusion fEIT
Aeration change	Volume-difference fEIT	ΔEELV, ΔEELZ, ΔEELI
Respiratory system mechanics	fEIT of dynamic C_{rs}	
	fEIT of quasi-static C_{rs} and landmark pressure points	fEIT of lower and upper inflection point pressures
	fEIT of opening / closing pressures	
	Regression fEIT	Linear regression fEIT, slope fEIT, filling capacity, polynomial fit fEIT, regional curvilinearity fEIT, filling index
	Time constant fEIT	
Ventilation timing	Ventilation delay fEIT	Opening / closing delay
	Expiration time fEIT	
Tissue classification	fEIT of overdistension / atelectasis	
	Low tidal variation fEIT	Silent spaces

Abbreviations: C_{rs}, respiratory system compliance; EELI, end-expiratory lung impedance; EELV, end-expiratory lung volume; EELZ, end-expiratory lung impedance; FEF_{25}, forced expiratory flow at 25% of FVC exhaled; FEF_{75}, forced expiratory flow at 75% of FVC exhaled; fEIT, functional EIT; FEV_1, forced expiratory volume in 1 s; IVC, inspiratory vital capacity; FVC, forced vital capacity; TV, tidal variation; V_T, tidal volume; Δ, change.

Figure E4.3 provides an overview of these types of fEIT images, based on a set of maneuvers or interventions during EIT data acquisition. During an initial PEEP setting, a subject is ventilated and fEIT measures of (A) ventilation and C_{rs}, and (B) delays and

respiratory time constants are calculated. A new PEEP setting is then applied and fEIT measures of (C) changes in aeration (e.g. in end-expiratory lung volume (ΔEELV)) are calculated. Last, a pressure-volume (P-V) loop is performed, from which (D) other fEIT parameters of respiratory system mechanics are calculated.

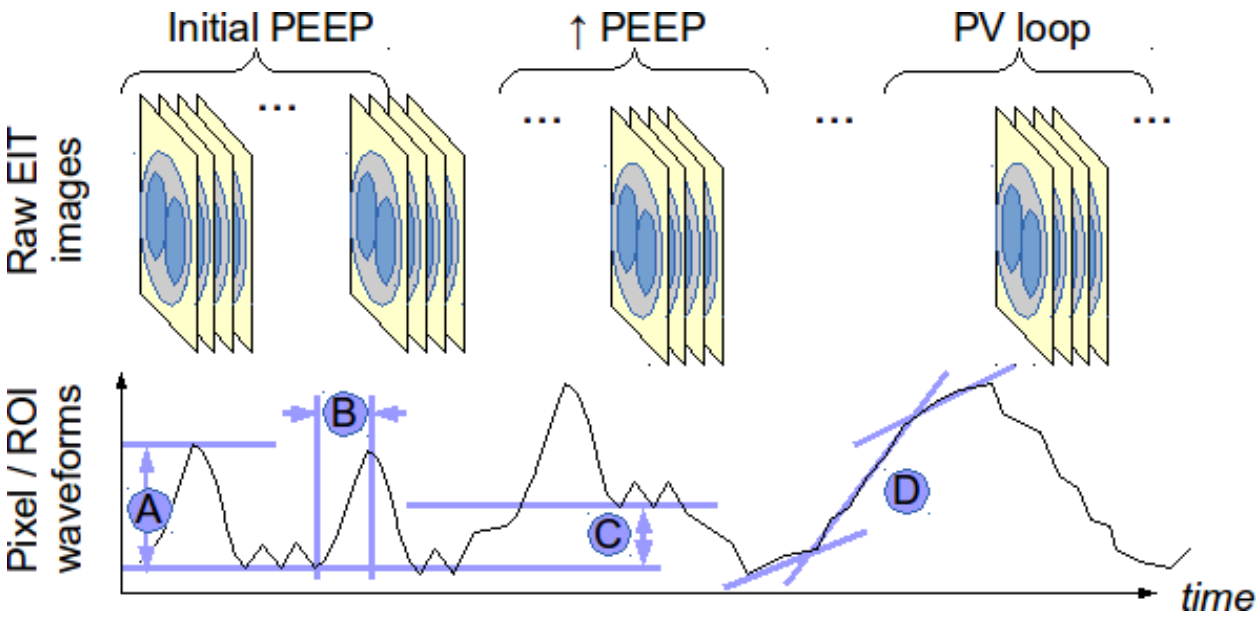

Figure E4.3. Conceptual diagram of the types of fEIT images, based on raw images acquired during an initial PEEP setting, an increased PEEP and a quasi-static pressure-volume (P-V) inflation and deflation maneuver. Each letter indicates the type of fEIT images: A) measures of the distribution of ventilation and of regional compliance (the illustration shows a measure of tidal variation), B) measures of regional delays and time constants (the illustration shows a measure of inspiratory time), C) measures of regional changes in aeration due to an intervention (the illustration shows a slow inflation), and D) measures of PV loop parameters (the illustration shows maximum curvature-change points).

fEIT images of ventilation distribution

One of the key advantages of EIT is its ability to provide real-time information on the distribution of ventilation. Thus, the earliest (and still most common) use of fEIT was to characterize the distribution of ventilation. Several different fEIT approaches have been developed, which we discuss below.

- **Standard deviation fEIT images**

The first type of functional EIT image presented in the literature is the standard deviation (SD) fEIT image (4). Each pixel of a SD fEIT image represents the SD of the data in the waveform of the pixel in the image sequence. This technique relies on the fact that the largest variation of impedance observed in a sequence of images is related to ventilation. Figure E4.4 illustrates a SD fEIT image. For each of the three black pixels, the corresponding waveforms are represented on the left. The middle histograms represent the distribution of impedance values for each waveform used to compute the SD value that is then assigned to the corresponding pixel in the functional image.

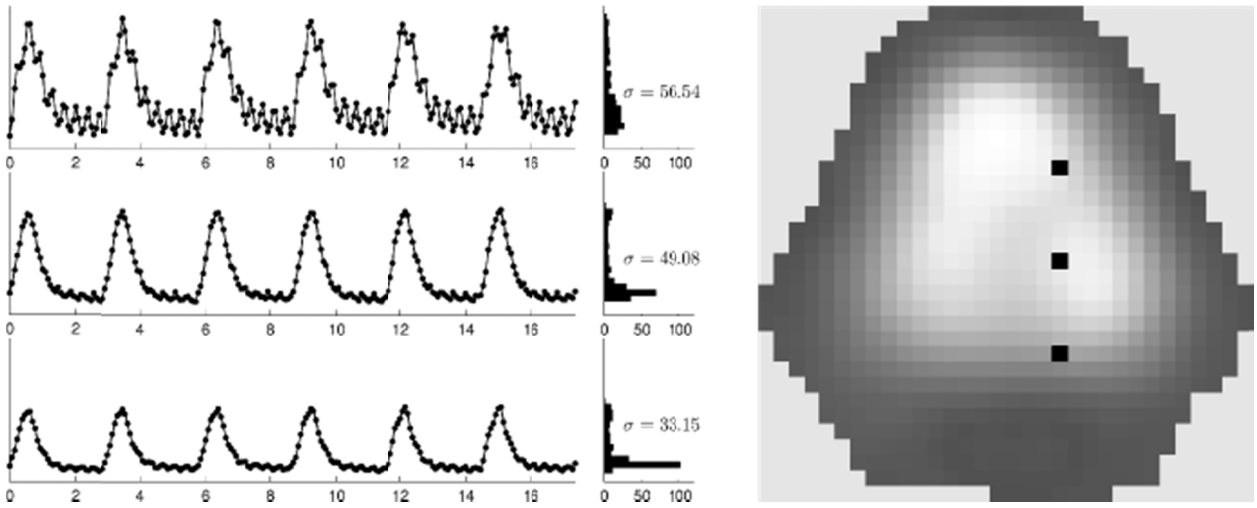

Figure E4.4. Standard deviation (SD) functional EIT image (right) obtained by calculating the waveform SD of individual pixels over the analyzed time period (left). On the left, the waveforms at the indicated pixel locations are shown. The histograms in the center column represent the distributions of impedance values for each pixel waveform. The distribution of values in each histogram can be characterized by a SD, σ, shown. These values are displayed as pixel values in the fEIT image (right). Note that the SD fEIT image relects both pulmonary and cardiogenic signal sources. This is seen in the upper waveform originating from the most anterior pixel close to the heart (top left).

This simple approach has the advantage of requiring little computational power and working well at slow scan rates, when only a few data samples (in time) are available for each breath, and was thus suitable for the early EIT devices, which were capable of generating only a few frames per second. While simple to calculate, there are a number of limitations to SD fEIT images. It is not a specific measure, and thus is unable to distinguish

ventilation-related changes in impedance from the cardio-synchronous ones, or artifacts in the data (caused e.g. by poor electrode contact). Additionally, since, by its calculation, SD is always positive, areas of increasing or decreasing air volume cannot be distinguished in such images.

- **Tidal variation fEIT images**

Tidal variation functional EIT (TV fEIT) images show the difference between EIT image values at end-inspiratory and end-expiratory times for each pixel of the functional image. The occurrences of end-inspiratory and end-expiratory events are typically automatically identified on a global waveform that is obtained by computing the sum of all pixels of the image sequence. The values of each pixel waveform at these time occurrences are then averaged for each of the end-inspiratory and end-expiratory events. Each pixel of the TV fEIT image is then calculated as the difference between its average end-inspiratory and average end-expiratory value (Figure E4.5). Each of the three black dot pixel values is obtained from the waveforms on the left. The red dots indicate the waveform values at each end-inspiratory event while the blue dots indicate the waveform values at each end-expiratory event. The red horizontal line represents the average of the end-inspiratory values while the blue line represents the average of the end-expiratory values. The difference between the red and the blue lines represents the pixel values in the TV fEIT image.

The advantage of this method is that it is specific to ventilation changes. It is more complicated computationally because the signal processing is required to identify the breath boundaries. While automatic approaches to detect end-inspiratory and end-expiratory events work well in many circumstances, they can occasionally give incorrect results when the pattern of ventilation is unusual or when there is a difference in phase of ventilation among regions. Incorrect detection of these breathing time points will disturb the fEIT images. One correction is for the human operator to review and correct these detections (e.g. (5)).

- **Normalized tidal variation fEIT images**

A "normalized tidal ventilation image" is an fEIT image in which TV image is normalized such that each image is represented as a fraction of the one with the maximum value. In this case, each image pixel is then a fraction or a percentage value. Such an image is useful to visually present the spatial pattern of the distribution of ventilation within the lung. This has also been referred to as the "stretch" fEIT image (6).

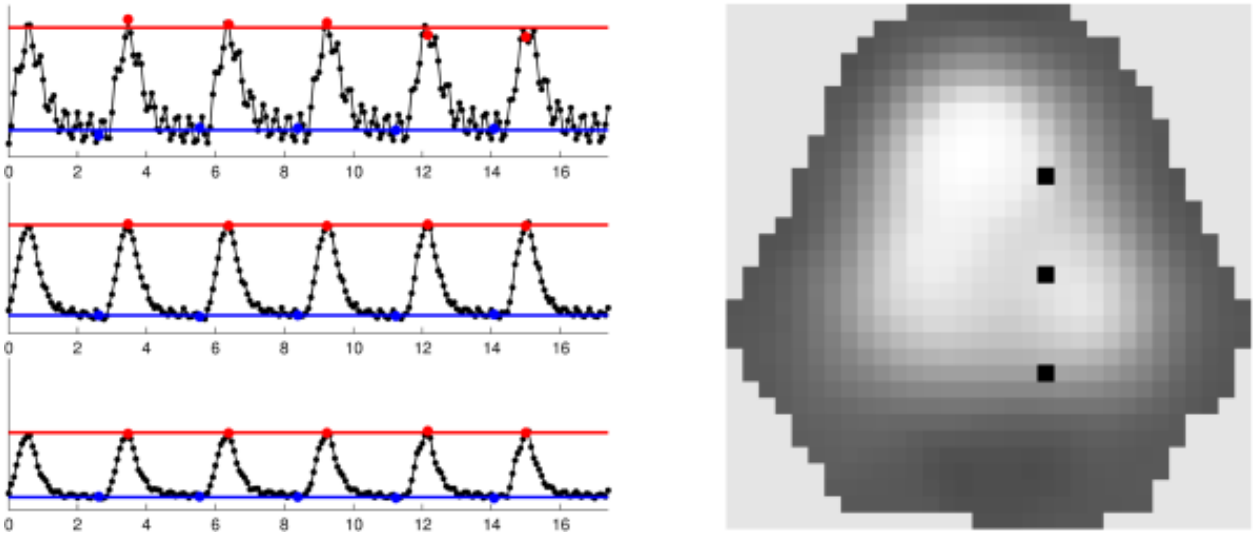

Figure E4.5. Tidal variation (TV) fEIT image (right). Time courses (left) from the indicated pixels are analyzed to determine the values at each end-inspiratory (red dots) and end-expiratory (blue dots) event, and subsequently averaged, yielding the red and blue lines. Each fEIT image pixel value is obtained by subtracting the values corresponding to the red and blue lines (also shown as a value of TV) and is visually expressed in the respective shade of gray of the pixels,

- **fEIT images of other lung volumes than V_T**

Regional ventilation distribution has mostly been examined by EIT during either spontaneous or mechanical tidal ventilation, with a focus on monitoring tidal breathing. However, it is also possible to analyze the distribution of other lung volumes in the chest cross-section than V_T. Virtually all lung volumes typically determined during conventional pulmonary function testing by spirometry as global values at the airway opening can be assessed by EIT on a regional level. The prerequisite is that the subjects are examined by EIT during well-known ventilation maneuvers like full inspiration and forced full expiration. The resulting pixel EIT waveforms are analyzed by calculation of differences between the impedance values at characteristic time points (e.g., full expiration to residual lung volume, full inspiration to total lung capacity with the onset of forced expiration and the end of forced full expiration). This allows the assessment of pixel lung volumes like inspiratory vital capacity (IVC), forced vital capacity (FVC), expiratory (ERV) and inspiratory reserve volumes (IRV) or forced expiratory volume in 1 s (FEV_1) (7-11). The distribution of these lung volumes is then visualized by plotting these values as fEIT.

- **fEIT images of ratios of lung volumes or flows**

Regional lung function is conventionally assessed not only by determining the lung volumes but also by several quotients determined as ratios between various lung volumes or between air flows. The best known are the ratios of FEV_1 and FVC or of maximum forced flow rates at defined volumes. These ratios can be determined by EIT in individual image pixels representing the chest cross-section. The corresponding fEIT images can be used to determine the spatial heterogeneity of ventilation.

A few clinical studies have been performed using this approach. For instance, EIT-derived FEV_1/FVC values acquired in patients suffering from chronic obstructive lung disease were not only significantly lower than in healthy subjects but they also exhibited a higher inhomogeneity of their spatial distribution (8). These measures were able to differentiate patients with asthma from age-matched controls (11) and to identify the regional effects of an inhaled bronchodilator during reversibility testing (10). The fEIT images of pixel ratios of forced expiratory flows after exhalation of 75% and 25% of FVC identified the spatial distribution of airway obstruction in patients with cystic fibrosis (12).

fEIT images using frequency analysis

As described in EOS 3, frequency filtering can be used to extract ventilation and cardiac-related information from EIT images. The underlying concept is to filter each EIT pixel waveform to extract only the signal at the breathing (and the cardiac, if desired) frequency, and then to measure the amplitude of this extracted signal. The breathing and heart rates are determined either 1) automatically, by analyzing the power spectrum of the global waveform – obtained by computing a Fourier Transform (FT) on the global signal and identifying the highest peak in the expected frequency range for breathing and heart rates or 2) from another instrument such as the patient ventilator, impedance plethysmograph, ECG or pulse oximetry. Once these rates are known, the FT of each waveform corresponding to individual pixels in the sequence of raw images is performed. The frequency signal amplitudes at the breathing and heart rates are then each assigned to a different fEIT image: the first corresponds to ventilation while the second represents heart-frequency related impedance changes. Figure E4.6 shows examples of fEIT images obtained by frequency analysis.

- **Ventilation-frequency fEIT images**

The frequency-analysis fEIT method has many advantages in its ability to identify and measure ventilation-related changes. It has a high specificity; by using a narrow, adapted filter centered on the breathing frequency, it is able to reject non-ventilation contributions to the fEIT image. However, there are also several practical challenges. First, it is sometimes difficult to identify the peak corresponding to the ventilation rate in the frequency spectrum, as it is not always the highest one. Second, it is not clear how harmonics of the main respiratory and heart rate should be analyzed, since only a fraction of the amplitude of the breathing signal is contained at the principle frequency component. (In a few studies, frequency filtering is performed using a low or band-pass filter with the 1^{st} and 2^{nd} harmonics of the breathing rate included (e.g. (13, 14)). Another difficulty with this method is its assumption of a stable breathing and cardiac frequency. This assumption of a stable breathing frequency is appropriate for some ventilation modes, but not for spontaneously breathing patients or for some support ventilation modes. It is, however, the method of choice for high-frequency oscillatory ventilation (HFOV), where the waveform is simpler but only a few data points per breath are available (e.g. (15, 16)).

- **Cardiac-frequency fEIT images**

Frequency-analysis fEIT can provide high quality images of the cardiac-related EIT image contributions. Since the cardiac-frequency contributions are much smaller and closer to the EIT frame rate, a very selective filter (such as provided by this technique) is required. Clearly, if the heart rate is not stable, frequency analysis will not be an appropriate analysis technique. Since this cardiac frequency-filtered image contains information on perfusion it has been called a "perfusion image" in some publications (e.g. (13, 17, 18)). However, there are several physiological reasons why the EIT image filtered at the cardiac frequency does not correspond directly to the perfusion. First, this analysis assumes a constant and stable heart rate, which may not be valid in most clinical scenarios. Next, overestimation of perfusion is possible, because the movement of the heart via cardioballistic effects independently contributes to EIT signals in addition to the perfusion contribution (19). Underestimation of perfusion is also possible, because small blood vessels (especially capillaries and veins in which blood flow is continuous) will not show a pulsatile component (20). This latter effect would also presumably be gravity dependent. We thus recommend, this type of fEIT image be referred to as "cardiac-related", "heart beat-related", "cardiac frequency-filtered" or the "pulsatility" fEIT image. If the cardiac frequency is a multiple of

the ventilation frequency, the cardiac frequency-filtered image also contains aliasing artifacts from ventilation as explained in EOS 3.

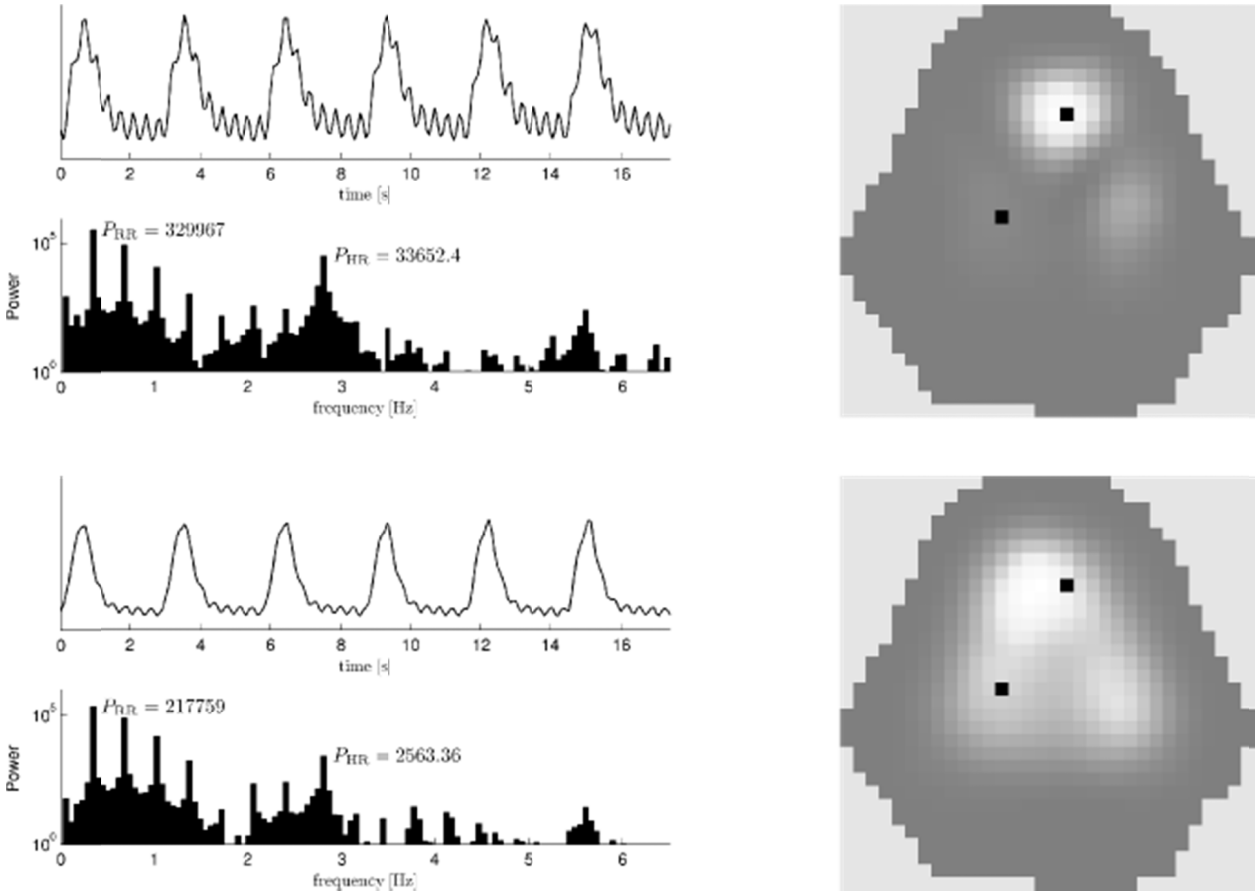

Figure E4.6. Functional EIT images obtained via frequency (spectral) analysis. In the images, two pixels are selected (black dots). The waveform at each pixel is plotted on the left (the upper frame shows the upper dot, in the heart region; the lower frame shows the lower dot, in the lung region). Underneath each waveform, the power spectrum density (bar graphs) of individual pixel waveforms (plots) is obtained via the Fourier transform. The height of the main peaks, corresponding to the respiratory and heart rates (in this case 0.34 Hz = 20.4 min^{-1} and 2.81 Hz = 168.6 min^{-1}, respectively) are used to calculate ventilation (bottom-right) and cardiac-related (top-right) functional images. The harmonics of the breathing frequency can be clearly seen starting at about 0.6 Hz, and the first harmonic of the cardiac frequency can be seen at about 5.7 Hz. PRR, power density at the respiratory rate; PHR, power density at the heart rate.

fEIT images of aeration change

When ventilation therapy is adjusted by increasing the tidal volume or PEEP or when a recruitment maneuver is performed, the underlying clinical objective is often to increase the aeration of the lung. To help predict the effectiveness of the therapy, it is useful to analyze the distribution of additional or lost gas volumes. Several fEIT approaches have been proposed to perform this calculation.

- **Volume-difference fEIT images**

Volume-difference fEIT images represent the change in lung volume at a particular point of the respiratory cycle (e.g. end-expiration) following an intervention, such as increase in PEEP. If the volume difference is taken between end-expiration before and after an intervention, the image is referred to as a "change in EELV", "ΔEELV", "end-expiratory lung volume difference" or "end-expiratory lung impedance" fEIT image.

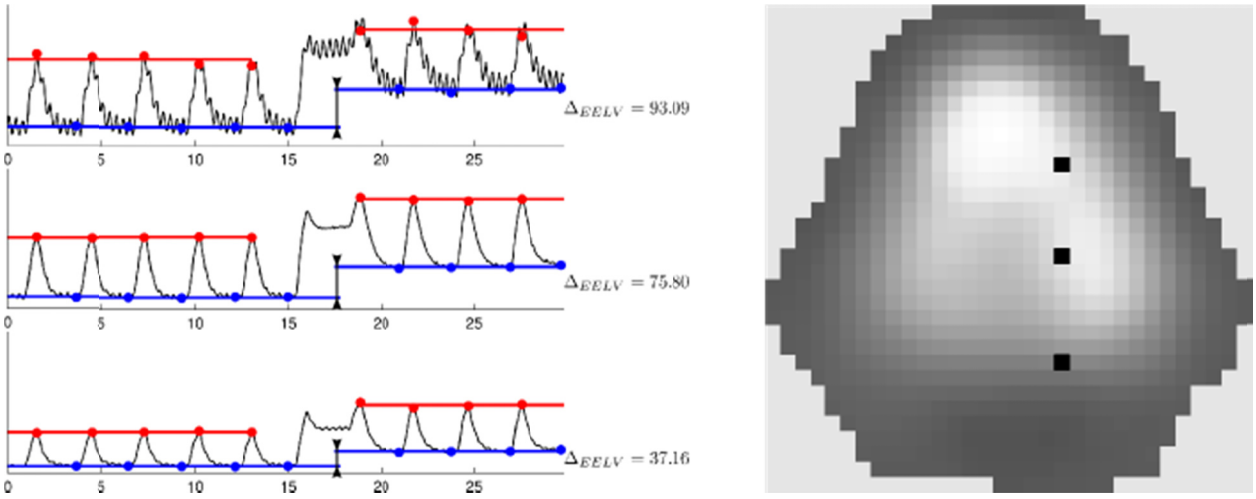

Figure E4.7. Image of change in end-expiratory lung volume (AU, right), due to a change in PEEP of 5 cmH_2O, as a function of time (s). In each indicated pixel in the image, a waveform is displayed (left), at which end-expiratory (blue dots) and end-inspiratory (red dots) time points are identified. The average end-expiratory value is calculated before and after the PEEP intervention (blue and red lines). Each pixel in the image (right) is then calculated from the difference in the values highlighted as blue lines before and after the intervention.

Figure E4.7 shows such an fEIT image. A global waveform is obtained by summing of all pixel values from a sequence of raw EIT images and is used to automatically identify end-

expiratory events. Based on the global EIT waveform, the time of each end-expiratory event is identified. Next, with each pixel waveform in the raw image sequences, end-expiratory values are identified at each identified end-expiratory time. End-expiratory values before and after the intervention are separately averaged, and then the difference between these two averages calculated. The functional image pixel values therefore reflect the increase or decrease in end-expiratory lung volume due to the intervention. An analogous calculation for the end-inspiratory event yields a functional image showing the change of the distribution of lung volume at end-inspiration. It should be noted that it is necessary for the calculation of any of these functional images that the same baseline (reference) measurement frame is used to reconstruct the difference EIT raw image before and after the intervention.

fEIT images of regional respiratory system mechanics

- **fEIT images of regional dynamic respiratory system compliance**

C_{rs} is a measure of the ease with which the chest wall and lung can increase in volume in response to an increase in airways pressure. Mechanical measurements of C_{rs} are thus in units of L/cmH_2O. EIT has seen much interest due to its potential to calculate regional measures of C_{rs}. Such an image of the regional distribution of C_{rs} provides useful information on the mechanical properties of lung tissue and can thus help guide therapeutic interventions. Unfortunately, it is not possible in vivo to calculate the regional micromechanical volumes and pressures from which true regional C_{rs} could be calculated. For lung pressure values, it is typical to assume that pressure is uniform throughout the lung, and to use the pressure reading from a ventilator when flow values have reached zero at both end-expiration and end-inspiration; this assumption may not be valid with obstructive lung diseases, especially if there were regions of trapped gas.

fEIT images of regional C_{rs} interpret gas volume as proportional to the EIT signal. This can be either the EIT image (in arbitrary EIT image units, AU) (1) or with the raw EIT image calibrated to some external measure of regional volume or global lung volume has been sometimes used (e.g. (21-23)). In all cases, measurements of incremental changes of lung volume and pressure are required to calibrate fEIT images of regional C_{rs}. Without calibration, such fEIT images would be considered to be images of ventilation.

Regional dynamic C_{rs} has often been determined from single breaths under dynamic ventilation conditions during an incremental and decremental PEEP trial (1, 22) and used to assess regional alveolar recruitment and overdistension. It can identify the PEEP step at which the most homogeneous distribution of regional C_{rs} occurs.

It is worth noting that fEIT images of aeration change also provide an approximation of C_{rs}, when normalized by the difference in airway pressure between peak-inspiration and peak-expiration.

- **fEIT images of regional quasi-static respiratory system compliance**

The quasi-static pressure-volume (P-V) maneuver is a standard tool to study respiratory system mechanics. As the lung inflates it changes from an initial low compliance (due to collapsed or atelectatic regions) through a region of high compliance and finally returns to a low compliance behavior (due to overdistension). The P-V curve is also able to measure the hysteresis of lung properties when acquired during both inflation and deflation. EIT data acquired during a P-V curve can provide regional functional information which can enhance the clinical value of the procedure. Figure E4.8 illustrates the types of information available from an EIT measurement during a P-V curve maneuver.

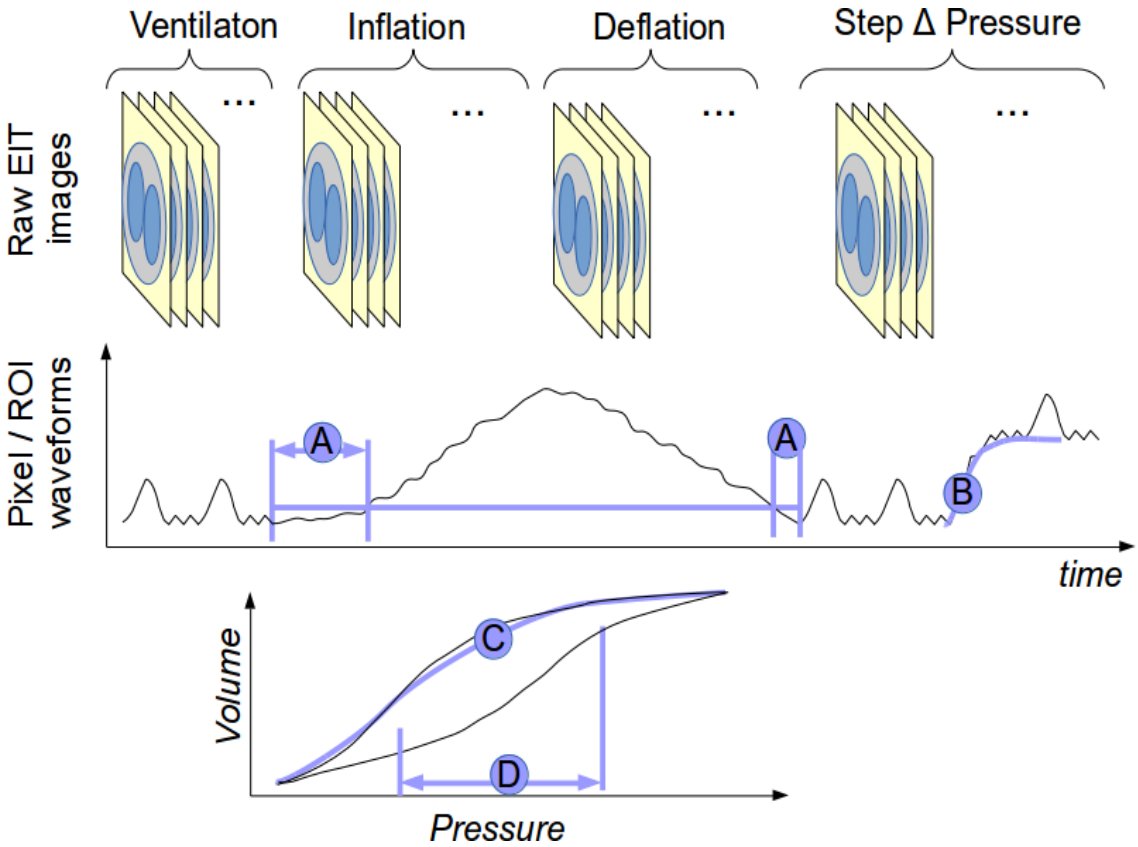

Figure E4.8. Illustration of the fEIT measurements available from data during a quasi-static constant low-flow inflation and deflation P-V maneuver. The top row shows raw EIT images during a period of ventilation, followed by inflation, deflation and then continued ventilation. The middle row shows representative EIT waveforms, and the bottom row volume (calculated from the EIT waveform, either calibrated to volume units, or in units of raw EIT impedance changes (ΔZ)). Parameter types which can be measure are illustrated: A) time to

cross a threshold fraction of the total ΔZ (which may be represented as an opening or closing pressure), B) time constant of an exponential curve fit to a step change in airway pressure, C) sigmoid curve fit to the P-V loop hysteresis, and D) maximum curvature-change values from the fitted curve (also referred to as "inflection" points).

When EIT data are recorded simultaneously with airway pressure either during a constant low-flow or a stepwise P-V maneuver, a quasi-static pressure-impedance curve is obtained for each pixel. Kunst et al. were the first to study fEIT measures from P-V curves using a low-flow inflation protocol, and used the data to estimate upper (UIP) and lower inflection points (LIP) in the EIT curves (24). A similar approach was used by van Genderingen et al. (25). Further work was done by Frerichs et al who fit the sigmoid curves of both inflation and deflation to EIT data from quasi-static P-V loops obtained in experimental animal with healthy, acutely injured and surfactant-treated lungs (26). Grychtol et al. proposed a method to automatically extract LIP and UIP, as well as C_{rs} assessment from such curves (27). Miedema et al. generated deflation pressure-impedance curves before and after surfactant treatment in high-frequency oscillatory ventilated preterm infants (28).

Note that the term "inflection point", while commonly used, is in fact mathematically incorrect. The points of interest are those at which a maximum change in slope of the curve occurs, but this is not an "inflection" (which is a change in curvature from positive to negative). Instead, we recommend the terminology "maximum curvature-change points".

- **Opening/closing pressure fEIT images**

As the lungs inflate from a low volume state, parts of the lung begin to open, and, similarly, as the lungs deflate, parts of the lung can close. A functional image of the pressures at which these events occur is a "regional opening (or closing) pressure fEIT image". In patients with acute respiratory distress syndrome, such images show significant heterogeneity, which may help to guide therapy.

In (5), regional opening and closing pressures were defined through a low-flow inflation and deflation maneuver. As the lungs were slowly inflated (allowing the pressure in lung regions to equalize to quasi-static conditions), the waveform in each image pixel was analyzed to determine when it began to increase from baseline (opening pressure) or when it returned to baseline (closing pressure). In this work, regional opening and closing pressures in each pixel were defined by the crossing of a threshold value in each pixel of the EIT image sequence, above which the lung region corresponding to that pixel is considered

open. A functional image of regional opening or closing pressure is then composed by assigning each pixel the value of airway pressure at the moment at which that threshold is crossed, respectively during inflation or deflation. This work defined the threshold in each pixel as a percentage (commonly 10%) of the total magnitude of changes recorded in that pixel during a respiratory cycle. Results based on (5) are shown in Figure E4.9.

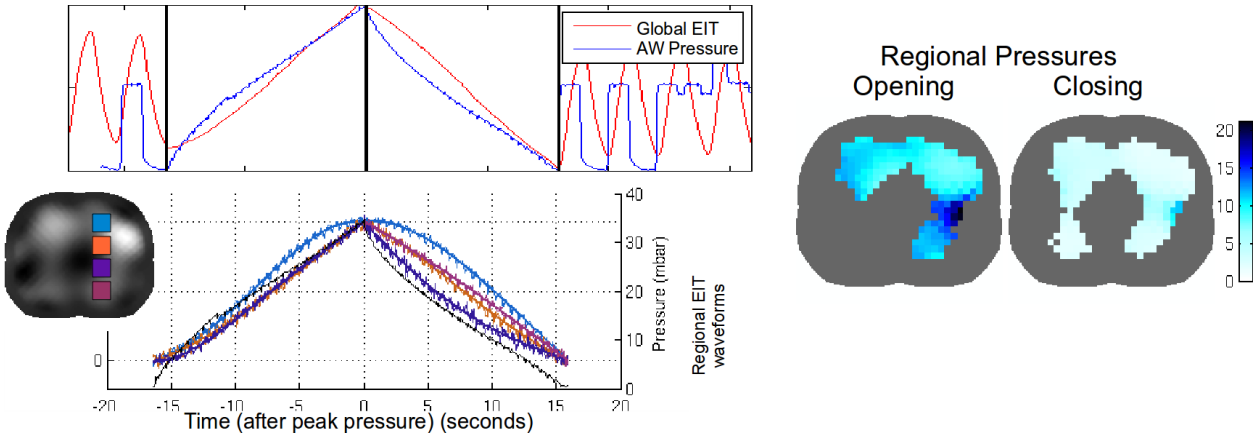

Figure E4.9. Calculation of regional opening and closing pressures fEIT images (5). Data were from slow-flow inflation and deflation on a patient with acute respiratory distress syndrome. The normalized global EIT and airway pressure (upper left) are shown, as well as the EIT waveform at four pixels in the image (colored lines, lower left). Based on the time of crossing a threshold, fEIT images of regional opening and closing pressures (units of cmH_2O) are shown.

It is possible to calculate opening and closing pressure fEIT images for each breath during conventional ventilation (given a sufficiently high scan rate); however, such dynamic conditions would not permit the assumption of quasi-static pressures in the lungs. An fEIT showing regional opening pressure during tidal breathing is shown in Figure E4.10.

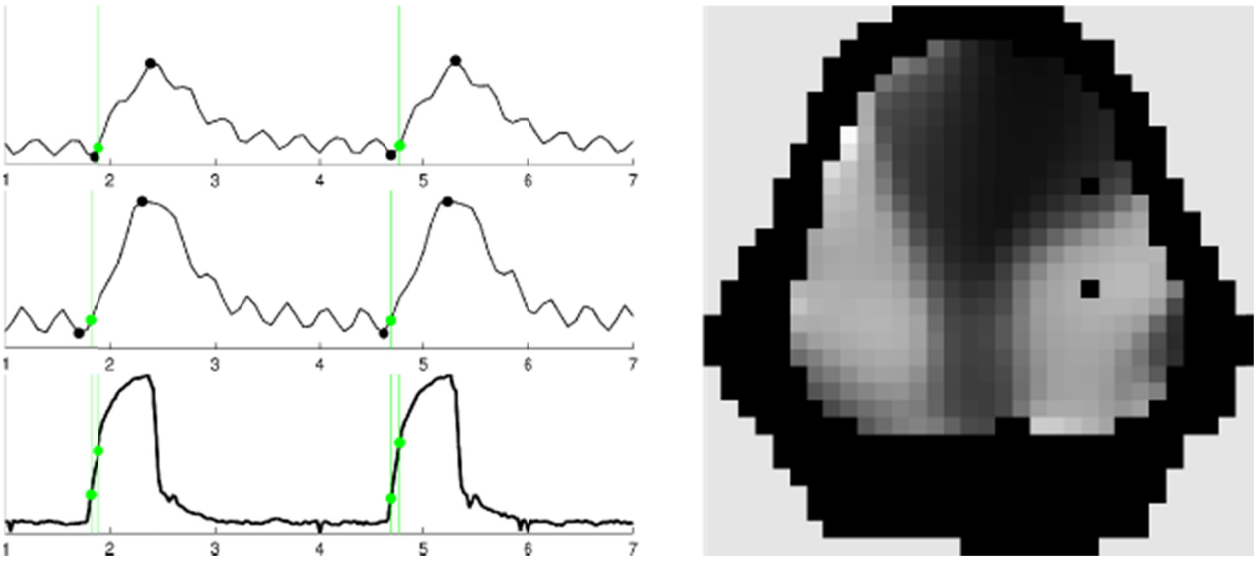

Figure E4.10. Regional opening pressure fEIT image (right). For the indicated image pixels (dark spots), the waveforms are shown at left during conventional ventilation. After end-expiration (black dot), the moment at which an individual waveform (top left) reaches 10% of its maximum tidal change (or overall change determined through a low-flow inflation maneuver) is identified (green dot) and the corresponding value of instantaneous airway pressure (bottom left) is used to compose a functional image (right). Pixels exhibiting tidal changes less than half the average were excluded (set to black). Brighter colors indicate lower opening airway pressures.

- **Regression fEIT images**

If a measure of pressure synchronous with the EIT signal is not available, it is possible to calculate a regression functional EIT image, which gives a compliance measure based on a linear fit of regional to global measures. Regression fEIT images are obtained by performing a regression analysis between the waveform of each pixel from a sequence of raw EIT images and the global waveform. This technique was developed by (29) and initially called "Filling capacity". It is described in detail by (30, 31). While the original terminology is still used, we recommend the terminology "regression fEIT image".

In a regression fEIT image, each pixel represents the slope of the regression relationship between each individual pixel waveform and the global waveform, thus representing each pixel's average contribution to the global waveform. It is not uncommon for some pixels to show a small negative slope, meaning that their value decreases as the global value increases. Such pixels are usually assumed to lie outside the lung ROI (see EOS 3) but in specific situations such as one-lung ventilation, they may be located in the

(contralateral) lung region as well (30). Figure E4.11 represents a regression fEIT image. While linear regression is commonly used, polynomial regression is also possible in cases where the lung filling or emptying characteristics are very non-linear (32, 33). The curvilinearity of lung filling has also been described by fitting an equation of the form of $Z=a\cdot Z_{glob}^{FI}+c$ to the EIT waveforms on a pixel-by-pixel basis (34, 35). (Z is pixel impedance, Z_{glob} global impedance, a and c constants, and FI the filling index.)

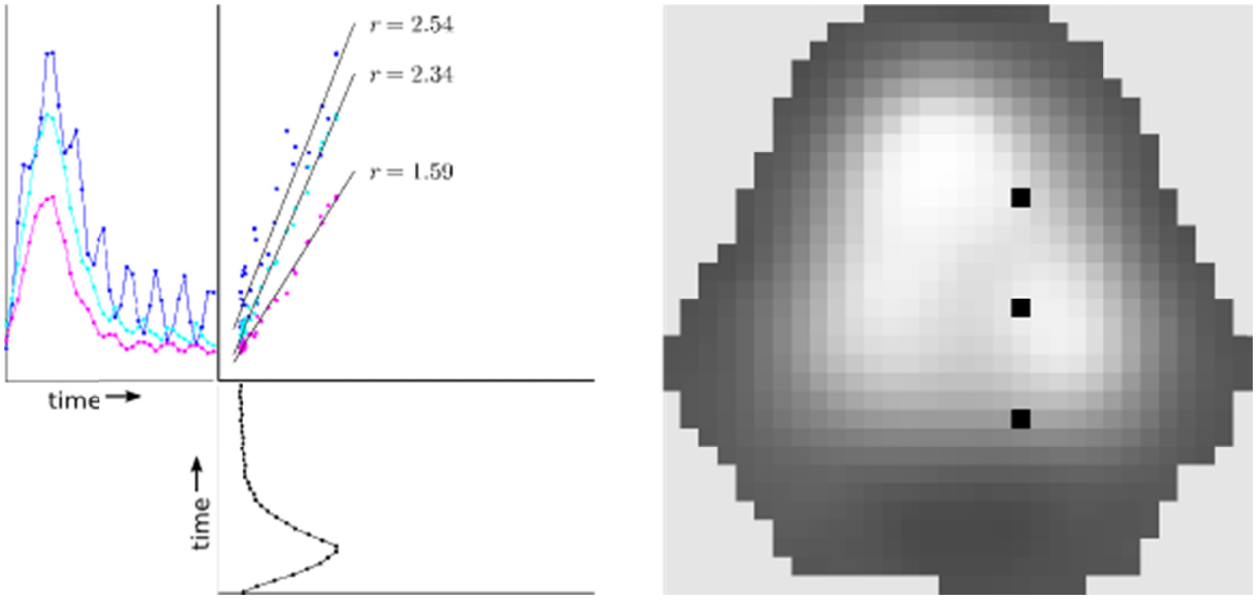

Figure E4.11. Regression fEIT image (right). For three image pixel locations (indicated), the pixel waveform is plotted as a function of time (left) and the global waveform is plotted below (left, bottom, rotated and reflected). In the left center, time points on the pixel and global waveforms are plotted and the best linear fit calculated. For each line, the value of the regression slope, *r,* is indicated. The fEIT image (right) is displayed, using the linear regression slope as the value for each pixel.

- **Time constant fEIT images**

A time constant characterizes the rate of relaxation of a system after a change. A linear system with a resistive and elastic element will respond to a step change with an exponential relaxation. The most common models of lung tissue consider the tissue to have mechanical properties characterized by a compliance and resistance, and thus respond to pressure and volume changes with a time constant, τ, proportional to resistance and compliance. The spatial distribution of time constants in a fEIT image thus provides useful information on the spatial distribution of lung mechanical properties. One example of the

use of such images is to visualize the effects of surfactant treatment on the regional dynamic tissue properties (36, 37).

To obtain time constant fEIT images, EIT data should be recorded before and after a step increase or decrease in airway pressure is performed (36). An exponential decay curve ($y = y_0 e^{-t/\tau}$) is then fitted to the EIT waveform after the pressure increase or decrease for each pixel. The time constant τ is then calculated to each pixel value to form the time constant fEIT image. Time constant analysis was also used by Miedema et al. who performed small incremental and decremental pressure steps in preterm infants receiving HFOV and analyzed the time constant of adaptation in the EIT signal in global, ventral and dorsal regions (37). Time constants may be calculated for other physiological phenomena in the lungs, including for the inspiratory and expiratory phase of each breath (38).

fEIT images of ventilation timing

- **Ventilation delay fEIT images**

Regional ventilation delay measures a similar property to regional opening and closing pressures. Lung regions which are less compliant will respond more slowly to an applied pressure step and will begin opening later than more compliant regions. Regions with large ventilation delays may thus be considered pathological, and the corresponding fEIT images should provide a useful guide to therapy (39).

The regional ventilation delay fEIT image represents the regional ventilation delay compared to the global waveform. Figure E4.12 represents a regional ventilation delay functional EIT image for one breath obtained from a ventilated pig. The pixel values are obtained by first finding, for each breath, the instant where each corresponding pixel waveform reaches a threshold of its overall magnitude as defined by its end-expiratory and end-inspiratory values. (Threshold values of up to 40% were used (39)). Where the threshold was crossed at an instant between two EIT data samples, the estimate is calculated by interpolation of the EIT waveform (using linear or higher order interpolation). The same process of finding the instant where the values reach a threshold of the overall magnitude is performed on the global waveform. The regional ventilation delay pixel values correspond to the difference between each individual waveform and the global waveform. A negative value means that the corresponding ventilation in this pixel leads the average ventilation while a positive value means that the ventilation in this pixel is lagging the average ventilation.

Regional ventilation delay can be calculated from data collected during conventional ventilation; however, the calculated image will then represent the lung pressures under dynamic conditions. To calculate delays under quasi-static conditions, a large constant low-flow breath (e.g. inspiratory gas flow 4 L/min, or tidal volume 12 mL/kg predicted body weight) can be performed to increase pressure resolution and minimize the effect of airway resistance. As mentioned, regional ventilation delay and opening-pressure fEIT images are calculated in similar ways. Both calculations seek the point at which the EIT waveform crosses a threshold; however, the opening-pressure fEIT image is then mapped on the corresponding pressure, while the regional ventilation delay image is presented in units of time.

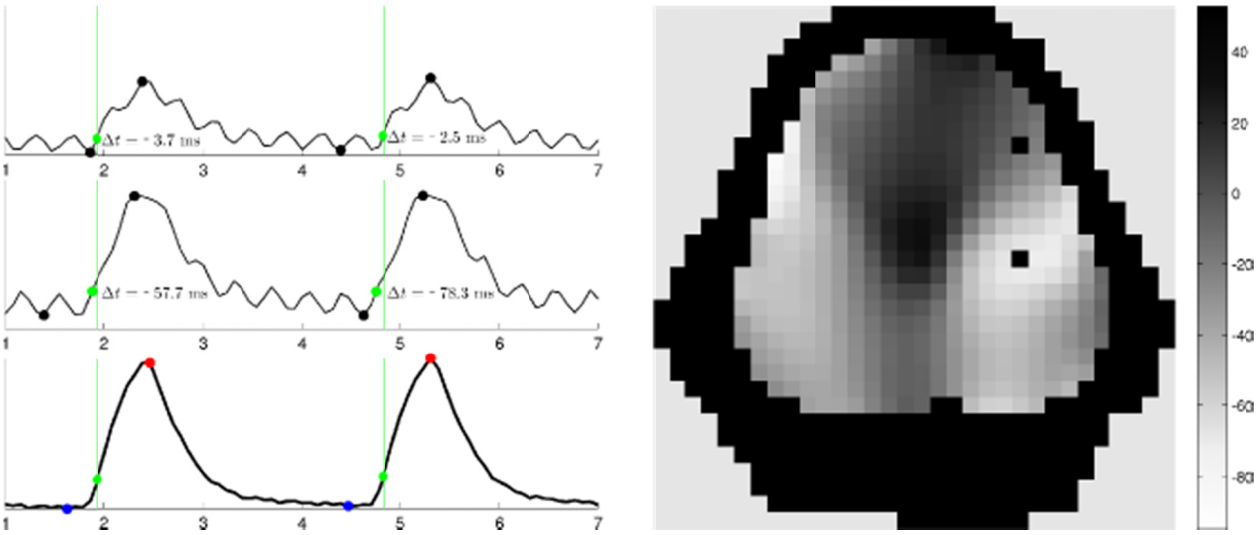

Figure E4.12. Regional ventilation delay EIT functional image (right). Two image pixels (dark spots in the image) are selected, and the waveform shown at left (left top two panels). The global EIT waveform is shown (bottom left) for which minimum end-expiration values (blue dots) are determined. The time for the global waveform to cross a threshold (20% of its maximum excursion) is determined and represents a delay of zero (see color axis at right). Each pixel waveform is then analyzed to determine the time required (green dots) for an individual pixel (top left) to reach 20% of its overall magnitude change in each breath (green line). The fEIT image is then the time difference between each pixel ventilation delay and the global delay. Blue and red dots mark the moment of maximum expiration and inspiration, respectively, while black dots mark the extrema for individual pixels in each breath cycle. Color axis on image is in milliseconds. Pixels with tidal change lower than half the average tidal change were excluded (blacked out).

In the presence of lung collapse, atelectatic areas may open up during inspiration and collapse again during expiration, a phenomenon called tidal recruitment. Wrigge et al have shown that the time-dependency of regional filling quantified as regional ventilation delay correlates with tidal recruitment (40).

- **Expiration time fEIT images**

Calculation of pixel expiration times can also be applied to assess the temporal heterogeneity of ventilation. This approach has been applied in spontaneously breathing subjects examined by EIT during conventional pulmonary function testing. The pixel expiration times needed to exhale defined fractions (25%, 50%, 75% and 90%) of FVC during forced full expiration were shown to be a robust measure to determine the high temporal heterogeneity of exhalation in patients with airway obstruction (8, 10, 11).

fEIT images with classification of regional lung tissue state

Different types of functional EIT image may be jointly analyzed to diagnose regional lung (patho-) physiology. Of particular clinical interest is the identification of hyper- or (over-) distended and atelectatic lung regions, as this provides clinically useful physiological information.

- **fEIT images of regional overdistention and atelectasis**

Both ovedistended and atelectatic regions are characterized by low C_{rs}, and thus low tidal impedance change. They differ in that an increase in airways pressure may open a collapsed area, leading to its opening and hence an increase in C_{rs}, whereas in an overdistended lung region increased pressure leads to a further reduction of C_{rs}.

Based on this difference, two approaches for identifying lung tissue were proposed (27, 41). Costa et al. analyzed changes in functional images of C_{rs} during a PEEP titration (41). Using the assumption that airway pressure is uniform throughout the lung, local C_{rs} is calculated by dividing local tidal change by the difference in airway pressure between peak-inspiration and peak-expiration. The amount of collapse or overdistention in the lung area corresponding to each pixel is quantified by comparing its C_{rs} at a given PEEP level with the best C_{rs} observed throughout the maneuver. This approach was also described in (42). In (23) it was used to guide choice of PEEP settings in management of experimental lung injury.

The approach of (27) is conceptually similar, but does not require a full titration maneuver. Instead, a single step increase in PEEP is used by a fuzzy logic expert system to identify lung areas which have become more open or more overdistended (or more collapsed or less overdistended for case of a decrease in PEEP). Rather than assuming uniform airway pressure, functional images of tidal changes were analyzed in tandem with volume change images to determine the direction of each pixel's movement along its P-V curve, and thus allow detection of the events of interest.

- **fEIT images of low tidal variation**

A simple approach to tissue classification is to determine all lung regions which have no – or very small – contribution to the global image amplitude. The approach of (6) identified so called "silent spaces" as those image pixels in which the normalized TV is less than a threshold of 10%. We propose the terminology "low tidal variation" regions as a more general synonym for "silent spaces". The advantage of this approach is its simplicity over a classification into collapsed or overdistended categories, since a lung region with low TV may have many possible causes, including overdistension, collapse or pneumothorax.

Robustness of fEIT approaches

Functional imaging approaches are an exciting aspect of EIT image analysis, since these images provide the connection between the raw EIT waveforms and the regional behavior of lung tissue. There is an active development of fEIT strategies to make them more robust and clinically useful. One key question in the selection of fEIT approach is the extent to which a given approach is sensitive to the sources of noise and artefact (e.g. low electrode contact quality) that may occur in EIT signals. There is clear evidence that some fEIT strategies are more robust than others. Pulletz et al. studied the impact of fEIT on the quantitative assessment of ventilation distribution (30). Hahn et al. compared their response to noise in a simulation study (31).

To illustrate these differences, the figure E4.13 compares three types of fEIT calculations used to measure regional ventilation amplitude, and described in the sections above: SD, regression and TV fEIT images. When EIT raw data are of high quality and interference is low, all these types of fEIT deliver similar images (Figure E4.13, top). However, real EIT measurements, especially over prolonged times, often show sources of interference (Figure E4.13, bottom). In this case, the most robust is the calculation of TV

fEIT images, since this type of fEIT updates its baseline with every breathing cycle by subtracting end-expiratory EIT images from end-inspiratory images. Hence, it can reduce the errors caused by measurement drift (Figure E4.13, bottom right).

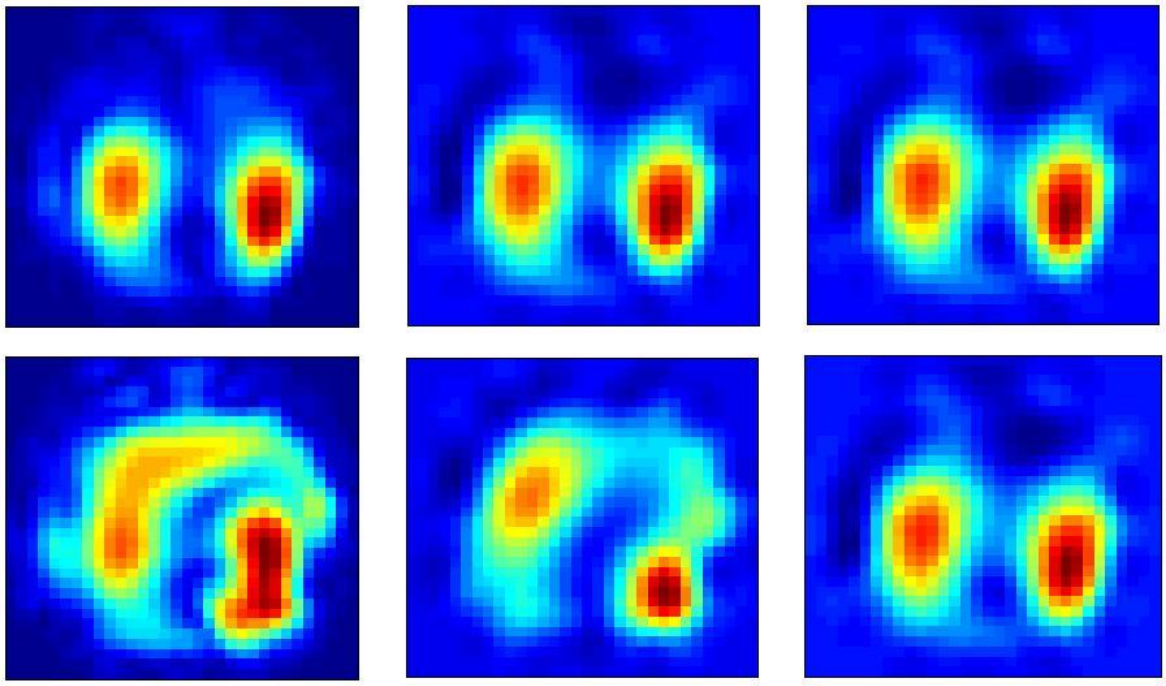

Figure E4.13. Comparison of fEIT images of regional ventilation amplitude calculated from EIT measurements on a patient during long-term monitoring during weaning. Three image calculations are shown: standard deviation fEIT (left column), regression fEIT (middle column), and tidal variation fEIT (right column). The top row shows images for the same data set, over a short period when no signal drift was present. The bottom row shows a subsequent long period with drift in the raw data (e.g. change of contact impedance, electrode movement). While all fEIT approaches appear similar without signal drift, the tidal variation fEIT with continuously updated baseline is the most robust in the presence of drift.

Document preparation

The first draft of this online document was prepared by B. Grychtol, Z. Zhao, A. Adler and I. Frerichs with collaboration of H. Wrigge. It was reviewed and approved by all other authors and collaborators.

References

1. Dargaville PA, Rimensberger PC, Frerichs I. Regional tidal ventilation and compliance during a stepwise vital capacity manoeuvre. *Intensive Care Med* 2010;36:1953-1961.
2. Frerichs I, Hahn G, Schroder T, Hellige G. Electrical impedance tomography in monitoring experimental lung injury. *Intensive Care Med* 1998;24:829-836.
3. Meier T, Luepschen H, Karsten J, Leibecke T, Grossherr M, Gehring H, Leonhardt S. Assessment of regional lung recruitment and derecruitment during a PEEP trial based on electrical impedance tomography. *Intensive Care Med* 2008;34:543-550.
4. Hahn G, Šipinková I, Baisch F, Hellige G. Changes in the thoracic impedance distribution under different ventilatory conditions. *Physiol Meas* 1995;16:A161-173.
5. Pulletz S, Adler A, Kott M, Elke G, Gawelczyk B, Schadler D, Zick G, Weiler N, Frerichs I. Regional lung opening and closing pressures in patients with acute lung injury. *J Crit Care* 2012;27:323 e311-328.
6. März A, Ukere A, Wodack K, Trepte C, Waldmann A, Böhm SH, Reuter D. Perioperative assessment of regional ventilation during changing body positions and ventilation conditions by electrical impedance tomography with increased spatial resolution and signal quality. *Critical Care* 2015;19 (Suppl 1):P249.
7. Vogt B, Falkenberg C, Weiler N, Frerichs I. Pulmonary function testing in children and infants. *Physiol Meas* 2014;35:R59-90.
8. Vogt B, Pulletz S, Elke G, Zhao Z, Zabel P, Weiler N, Frerichs I. Spatial and temporal heterogeneity of regional lung ventilation determined by electrical impedance tomography during pulmonary function testing. *J Appl Physiol* 2012;113:1154-1161.
9. Krueger-Ziolek S, Schullcke B, Kretschmer J, Muller-Lisse U, Moller K, Zhao Z. Positioning of electrode plane systematically influences EIT imaging. *Physiol Meas* 2015;36:1109-1118.
10. Vogt B, Zhao Z, Zabel P, Weiler N, Frerichs I. Regional lung response to bronchodilator reversibility testing determined by electrical impedance tomography in chronic obstructive pulmonary disease. *Am J Physiol Lung Cell Mol Physiol* 2016;311:L8-L19.
11. Frerichs I, Zhao Z, Becher T, Zabel P, Weiler N, Vogt B. Regional lung function determined by electrical impedance tomography during bronchodilator reversibility testing in patients with asthma. *Physiol Meas* 2016;37:698-712.
12. Zhao Z, Muller-Lisse U, Frerichs I, Fischer R, Moller K. Regional airway obstruction in cystic fibrosis determined by electrical impedance tomography in comparison with high resolution CT. *Physiol Meas* 2013;34:N107-114.

13. Frerichs I, Pulletz S, Elke G, Reifferscheid F, Schadler D, Scholz J, Weiler N. Assessment of changes in distribution of lung perfusion by electrical impedance tomography. *Respiration* 2009;77:282-291.

14. Tingay DG, Wallace MJ, Bhatia R, Schmolzer GM, Zahra VA, Dolan MJ, Hooper SB, Davis PG. Surfactant before the first inflation at birth improves spatial distribution of ventilation and reduces lung injury in preterm lambs. *J Appl Physiol* 2014;116:251-258.

15. Frerichs I, Achtzehn U, Pechmann A, Pulletz S, Schmidt EW, Quintel M, Weiler N. High-frequency oscillatory ventilation in patients with acute exacerbation of chronic obstructive pulmonary disease. *J Crit Care* 2012;27:172-181.

16. Wolf GK, Grychtol B, Frerichs I, Zurakowski D, Arnold JH. Regional lung volume changes during high-frequency oscillatory ventilation. *Pediatr Crit Care Med* 2010;11:610-615.

17. Smit HJ, Handoko ML, Vonk Noordegraaf A, Faes TJ, Postmus PE, de Vries PM, Boonstra A. Electrical impedance tomography to measure pulmonary perfusion: Is the reproducibility high enough for clinical practice? *Physiol Meas* 2003;24:491-499.

18. Fagerberg A, Stenqvist O, Aneman A. Monitoring pulmonary perfusion by electrical impedance tomography: An evaluation in a pig model. *Acta Anaesthesiol Scand* 2009;53:152-158.

19. Proenca M, Braun F, Rapin M, Sola J, Adler A, Grychtol B, Bohm SH, Lemay M, Thiran JP. Influence of heart motion on cardiac output estimation by means of electrical impedance tomography: A case study. *Physiol Meas* 2015;36:1075-1091.

20. Borges JB, Suarez-Sipmann F, Bohm SH, Tusman G, Melo A, Maripuu E, Sandstrom M, Park M, Costa EL, Hedenstierna G, Amato M. Regional lung perfusion estimated by electrical impedance tomography in a piglet model of lung collapse. *J Appl Physiol* 2012;112:225-236.

21. Lowhagen K, Lundin S, Stenqvist O. Regional intratidal gas distribution in acute lung injury and acute respiratory distress syndrome-assessed by electric impedance tomography. *Minerva Anestesiol* 2010;76:1024-1035.

22. Gomez-Laberge C, Rettig JS, Smallwood CD, Boyd TK, Arnold JH, Wolf GK. Interaction of dependent and non-dependent regions of the acutely injured lung during a stepwise recruitment manoeuvre. *Physiol Meas* 2013;34:163-177.

23. Wolf GK, Gomez-Laberge C, Rettig JS, Vargas SO, Smallwood CD, Prabhu SP, Vitali SH, Zurakowski D, Arnold JH. Mechanical ventilation guided by electrical impedance tomography in experimental acute lung injury. *Crit Care Med* 2013;41:1296-1304.

24. Kunst PW, Bohm SH, Vazquez de Anda G, Amato MB, Lachmann B, Postmus PE, de Vries PM. Regional pressure volume curves by electrical impedance tomography in a model of acute lung injury. *Crit Care Med* 2000;28:178-183.

25. van Genderingen HR, van Vught AJ, Jansen JR. Estimation of regional lung volume changes by electrical impedance pressures tomography during a pressure-volume maneuver. *Intensive Care Med* 2003;29:233-240.

26. Frerichs I, Dargaville PA, Rimensberger PC. Regional respiratory inflation and deflation pressure-volume curves determined by electrical impedance tomography. *Physiol Meas* 2013;34:567-577.

27. Grychtol B, Wolf GK, Adler A, Arnold JH. Towards lung EIT image segmentation: Automatic classification of lung tissue state from analysis of EIT monitored recruitment manoeuvres. *Physiol Meas* 2010;31:S31-43.

28. Miedema M, de Jongh FH, Frerichs I, van Veenendaal MB, van Kaam AH. Changes in lung volume and ventilation during surfactant treatment in ventilated preterm infants. *Am J Respir Crit Care Med* 2011;184:100-105.

29. Kuhnel G, Hahn G, Frerichs I, Schroder T, Hellige G. Neue Verfahren zur Verbesserung der Abbildungsqualität bei funktionellen EIT-Tomogrammen der Lunge. *Biomed Tech (Berl)* 1997;42 Suppl:470-471.

30. Pulletz S, Elke G, Zick G, Schadler D, Scholz J, Weiler N, Frerichs I. Performance of electrical impedance tomography in detecting regional tidal volumes during one-lung ventilation. *Acta Anaesthesiol Scand* 2008;52:1131-1139.

31. Hahn G, Dittmar J, Just A, Quintel M, Hellige G. Different approaches for quantifying ventilation distribution and lung tissue properties by functional EIT. *Physiol Meas* 2010;31:S73-84.

32. Frerichs I, Dudykevych T, Hinz J, Bodenstein M, Hahn G, Hellige G. Gravity effects on regional lung ventilation determined by functional EIT during parabolic flights. *J Appl Physiol* 2001;91:39-50.

33. Hinz J, Gehoff A, Moerer O, Frerichs I, Hahn G, Hellige G, Quintel M. Regional filling characteristics of the lungs in mechanically ventilated patients with acute lung injury. *Eur J Anaesthesiol* 2007;24:414-424.

34. Rooney D, Friese M, Fraser JF, K RD, Schibler A. Gravity-dependent ventilation distribution in rats measured with electrical impedance tomography. *Physiol Meas* 2009;30:1075-1085.

35. Grant CA, Fraser JF, Dunster KR, Schibler A. The assessment of regional lung mechanics with electrical impedance tomography: A pilot study during recruitment manoeuvres. *Intensive Care Med* 2009;35:166-170.

36. Pulletz S, Kott M, Elke G, Schadler D, Vogt B, Weiler N, Frerichs I. Dynamics of regional lung aeration determined by electrical impedance tomography in patients with acute respiratory distress syndrome. *Multidiscip Respir Med* 2012;7:44.

37. Miedema M, de Jongh FH, Frerichs I, van Veenendaal MB, van Kaam AH. Regional respiratory time constants during lung recruitment in high-frequency oscillatory ventilated preterm infants. *Intensive Care Med* 2012;38:294-299.

38. Róka P, Waldmann A, Müller B, Ender F, Bohm SH, Windisch W, Strassmann S, Karagiannidis C. Breath-by-breath regional expiratory time constants by electrical impedance tomography – a feasibility study. In: Sola J, Braun F, Adler A, editors. 16th International Conference on Biomedical Applications of Electrical Impedance Tomography. Neuchatel; 2015. p. 50.

39. Muders T, Luepschen H, Zinserling J, Greschus S, Fimmers R, Guenther U, Buchwald M, Grigutsch D, Leonhardt S, Putensen C, Wrigge H. Tidal recruitment assessed by electrical impedance tomography and computed tomography in a porcine model of lung injury. *Crit Care Med* 2012;40:903-911.

40. Wrigge H, Zinserling J, Muders T, Varelmann D, Gunther U, von der Groeben C, Magnusson A, Hedenstierna G, Putensen C. Electrical impedance tomography compared with thoracic computed tomography during a slow inflation maneuver in experimental models of lung injury. *Crit Care Med* 2008;36:903-909.

41. Costa EL, Borges JB, Melo A, Suarez-Sipmann F, Toufen C, Jr., Bohm SH, Amato MB. Bedside estimation of recruitable alveolar collapse and hyperdistension by electrical impedance tomography. *Intensive Care Med* 2009;35:1132-1137.

42. Gomez-Laberge C, Arnold JH, Wolf GK. A unified approach for EIT imaging of regional overdistension and atelectasis in acute lung injury. *IEEE Trans Med Imaging* 2012;31:834-842.